Advances in Applied Mathematics and Mechanics
Adv. Appl. Math. Mech., Vol. **7**, No. 5, pp. 549-568

DOI: 10.4208/aamm.2014.m538
October 2015

Numerical Study on the Dynamics and Oxygen Uptake of Healthy and Malaria-Infected Red Blood Cells

P. G. Jayathilake[1], Gang Liu[1], Zhijun Tan[3,*] and B. C. Khoo[1,2]

[1] *Department of Mechanical Engineering, National University of Singapore, Kent Ridge Crescent, Singapore 119260, Singapore*
[2] *Singapore-MIT Alliance, 4 Engineering Drive 3, National University of Singapore, Singapore 117576, Singapore*
[3] *Guangdong Province Key Laboratory of Computational Science and School of Mathematics and Computational Science, Sun Yat-sen University, Guangzhou 510275, China*

Received 13 March 2014; Accepted (in revised version) 7 November 2014

Abstract. Red blood cells (RBCs) are very important due to their role of oxygen transport from lungs. As the malaria parasite grows in the malaria-infected red blood cells (IRBCs), the properties of the cells change. In the present work, the oxygen uptake by RBCs and IRBCs at the pulmonary capillaries is simulated using a numerical technique based on the two-dimensional immersed interface method. The results for the oxygen uptake by a stationary single RBC have fair agreements with the previously reported results. The numerical results show that the malaria infection could significantly cause deterioration on the oxygen uptake by red blood cells. The results also suggest that the oxygen uptake by individual stationary RBC/IRBC would not be significantly affected by the neighboring cells provided the separation distance is about the dimension of the cell. Furthermore, it appears that the oxygen uptake by both RBCs and IRBCs is dominated by mass diffusion over the convection although the Peclet number is of the order of unity.

AMS subject classifications: 76Z05, 76M20, 76D05, 76R99, 65M06, 74F10, 92C10
Key words: Red blood cell, malaria, oxygen, biomechanics, numerical simulation.

1 Introduction

The human red blood cells (RBCs) play a very important role since they help to carry gases such as oxygen and carbon dioxide between alveolus and tissues. The biconcave

*Corresponding author.
Email: pgjayathilake@gmail.com (P. G. Jayathilake), mpeliuga@nus.edu.sg (G. Liu), tzhij@mail.sysu.edu.cn (Z. J. Tan), mpekbc@nus.edu.sg (B. C. Khoo)

RBC has an average diameter of 6-8μm and the life time is about 100-120days. The irregular deformation of RBCs and the change in mechanical properties may be responsible and associated with various diseases. As such, the study of the mechanical properties of RBCs and their deformation under different flow conditions has important implications on health.

The RBC shape is asymmetric when it flows along blood vessels. Secomb and Skalak [1] showed that the asymmetric motion of RBC results in the tank-treading motion of the RBC. The shape of the deformed cell may depend on many factors such as vessel diameter, cell velocity, cell membrane stiffness etc. [2]. Pozrikidis [3, 4] studied the RBC deformation and motion in shear and channel flows using the boundary integral method. Some other researchers have considered RBC aggregation too. Liu and Liu [5] numerically modeled RBC aggregation through a potential function, while Zhang et al. [6] studied the RBC aggregation under different shear rates. Varity of mathematical models have been developed to simulate RBCs [7].

Another class of research work on RBCs concerns the gas transfer by RBCs. Understanding gas transfer by RBCs is important to diagnose various pulmonary diseases and the design of effective drugs and treatments. In addition, the aforementioned knowledge is important to design efficient oxygenators and artificial lungs. As such, several researchers have been studying this problem for more than three decades. Hellums [8] studied the resistance to oxygen transport in the capillaries by modeling the capillary and RBCs simply as a circular tube and cylindrical slugs, respectively. Groebe and Thews [9] also modeled the RBCs as cylindrical particles and showed that the motion of RBCs could enhance oxygen release and make oxygen flux more uniform along the capillary. W ang and Popel [10] investigated the effect of the shape of RBC on oxygen transport and showed that the deformation of initial biconcave RBCs to "parachute" shape decreases spatially averaged oxygen flux.

One of the most infectious diseases affecting the circulatory system is the malaria. Each year about 1 million people die due to malaria. When healthy RBCs are infected by the malaria parasite, Plasmodium falciparum, the mechanical properties of cells are changed [12–14]. When the parasite matures in the malaria-infected red blood cells (IRBCs), the cells' membrane becomes stiffer and the deformability of the cells decrease significantly and hence exhibits difficulty in passing through capillaries [15]. Malaria infection produces knobs on the surface of the cells' membrane and these cause the membrane to become more adhesive. As such, IRBCs adhere to RBCs and endothelium cells which results in increasing flow resistant as reported in Kondo et al. [16]. Imai et al. [17] investigated the interaction between RBCs and IRBCs using a three-dimensional model and showed that IRBCs could marginalize during their interactions with a longer duration of contact with endothelium cells. Secomb et al. [18] used a theoretical model to examine the effect of glycocalyx on haematocrit and blood flow resistance. Also, Fedosov et al. [19] simulated the adhesive dynamics of IRBCs and revealed that IRBCs are flipped due to increased stiffness and the solid parasites inside the cells.

As mentioned earlier, when the malaria parasite matures inside an IRBC, the cel-

l membrane becomes stickier and stiffer causing the cell velocity to decrease [16]. As such, the oxygen transport by the RBCs would be deteriorated by the malaria infection [20]. Schall et al. [21] did experiments using western fence lizards and revealed that the haemoglobin concentration of RBCs of those lizards is decreased by 25% with malaria infection. Krishna et al. [20] also reported similar results by doing the experiments with mice. Krishna et al. [20] reported that the oxyhaemoglobin dissociation curve (ODC) of malaria infected mice shifted rightward. Furthermore, Bongbele et al. [22] examined the oxygen transport capacity of blood in athletes with malaria infection. The results showed that the malaria infection decreases the total number of RBCs, haemoglobin concentration and hematocrit too which causes the oxygen capacity of the blood to be greatly reduced.

To the best of authors' knowledge, numerical simulation of oxygen transport of IRBCs is perhaps not reported yet nor compared to that of RBCs. In the present work, RBCs and IRBCs are simulated separately/together using a two-dimensional numerical model based on the immersed interface method (IIM). The IIM is a second order accurate, sharp interface, and Cartesian grid numerical method successfully used to simulate deformable boundary problems [23]. Although the two-dimensional model differs from the real three-dimensional problem, it is believed that the model would provide some insight into the physiological function of the real biological system. The objective of this work is to investigate the deformation and oxygen uptake of IRBC compared with that of RBC. The rest of this paper is organized as follows. Section 2 describes the governing equations and numerical calculation procedure for a capsule-substrate adhesion problem (see Fig. 1). Section 3 presents the results and discussions on oxygen transport of a single RBC/IRBC stationary/flowing and multiple stationary cells in an arteriole, and Section 4 provides the conclusions for the present study.

2 Model formulation and numerical method

The following calculation procedure is discussed for a deformable RBC flowing along a vessel (Fig. 1). The elastic RBC and the surrounding environment (the lumen of the vessel) are filled with a Newtonian fluid. It is assumed that the fluid properties are the same for the RBC and the surrounding fluid (plasma).

2.1 Governing equations

The fluid motion is governed by the Navier-Stokes equations as given below:

$$\rho\Big(\frac{\partial\vec{u}}{\partial t}+\vec{u}\cdot\nabla\vec{u}\Big)=-\nabla p+\mu\nabla^2\vec{u}+\vec{F}, \tag{2.1a}$$

$$\nabla\cdot\vec{u}=0, \tag{2.1b}$$

where $\vec{u}=(u,v)$, p, and $\vec{F}$ are the fluid velocity, the fluid pressure, and the singular force at the interface, respectively. ρ and μ are the fluid density and dynamic viscosity, respec-

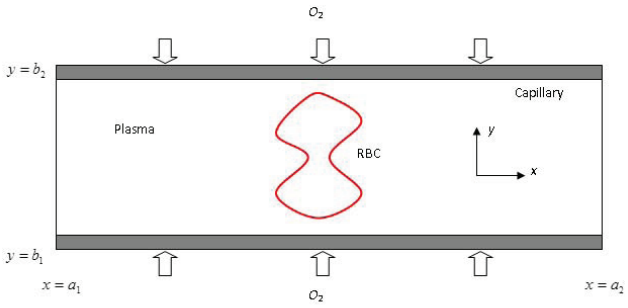

Figure 1: Schematic diagram for the mathematical model.

tively. The interfacial force is given by

$$F(\overrightarrow{x},t)=(F_1,F_2)=\int_\Gamma f(s,t)\delta(\overrightarrow{x}-\overrightarrow{X}(s,t))ds, \tag{2.2}$$

where $\vec{x}(x,y)$ is the spatial position, $\vec{X}(s,t)=(X,Y)$ is the membrane configuration Γ of the RBC, s is the arc length measured along the membrane, f is the force strength, and δ is the two-dimensional Dirac delta function. The force strength is given by

$$\vec{f}(s,t)=\frac{\partial}{\partial s}\left(T_e(s,t)\overrightarrow{\tau}(s,t)+T_b(s,t)\overrightarrow{n}(s,t)\right)+f_{ad}\vec{n}, \tag{2.3}$$

and the adhesive force is given by $f_{ad}=-\partial W/\partial y$. In this formulation, the adhesion potential is assumed as found in Seifert [24],

$$W=W_{ad}\left[\left(\frac{d_m}{y}\right)^4-2\left(\frac{d_m}{y}\right)^2\right], \tag{2.4}$$

where, W_{ad} is the adhesion strength and d_m is the minimum gap between the cell and the capillary walls. Following Zhang et al. [6], the neo-Hookean rheological properties are assumed for the membrane unless otherwise stated, and hence the elastic and shear tensions are, respectively, given as

$$T_e=E_e(\varepsilon^{1.5}-\varepsilon^{-1.5}), \tag{2.5a}$$

$$T_b=\frac{\partial}{\partial s}\left[E_b(\kappa-\kappa_R)\right]. \tag{2.5b}$$

Here, κ is the membrane curvature at any point while κ_R is the reference curvature. ε is the stretch ratio at any point of the membrane, E_e is the shear modulus of the membrane, and E_b is the bending modulus. The unit vectors, $\vec{\tau}$, $\vec{n}$ and $\hat{y}$ are defined at any point on the membrane, and their respective directions are in the anticlockwise tangential, the outward normal, and the y directions.

The oxygen transport in the plasma region satisfies the convection-diffusion equation as given below,

$$\alpha_P\Big(\frac{\partial P_{O_2}}{\partial t}+\vec{u}\cdot\nabla P_{O_2}\Big)=\alpha_P D_P\nabla^2 P_{O_2}, \tag{2.6}$$

where, P_{O_2}, α_P and D_P are the partial pressure of oxygen, solubility of oxygen in plasma, and diffusion coefficient of oxygen in plasma, respectively. The partial pressure of oxygen P_{O_2} is proportional to the corresponding oxygen concentration dissolved in the plasma, and hence $P_{O_2}=C_{O_2}/\alpha_P$, where C_{O_2} is the oxygen concentration. In the RBC, the following coupled equations are used to compute the oxygen distribution. These are

$$\alpha_R\Big(\frac{\partial P_{O_2}}{\partial t}+\vec{u}\cdot\nabla P_{O_2}\Big)=\alpha_R D_R\nabla^2 P_{O_2}-r, \tag{2.7a}$$

$$[Hb]\Big(\frac{\partial S_{O_2}}{\partial t}+\vec{u}\cdot\nabla S_{O_2}\Big)=[Hb]D_H\nabla^2 S_{O_2}+r. \tag{2.7b}$$

Here, α_R, D_R, $[Hb]$, DH, and S_{O_2} are the solubility of oxygen in RBC, diffusion coefficient of oxygen in RBC, the haemoglobin concentration, diffusion coefficient of haemoglobin in RBC, and the haemoglobin oxygen saturation in RBC, respectively. The reaction term r is the net carrier O_2 uptake rate (see [25]) given by

$$r=k[Hb]\frac{g(P_{O_2})-S_{O_2}}{1-g(P_{O_2})}, \tag{2.8}$$

where, $g(P_{O_2})$ is the oxyhaemoglobin dissociation curve (ODC). In consistent with other works [10], the reaction between oxygen and haemoglobin is assumed instantaneous and hence $S_{O_2}=g(P_{O_2})$. For the ODC, the Hill curve is assumed as commonly appeared in the literature [10] due to its simplicity. The Hill curve is given as

$$g(P_{O_2})=\frac{P_{O_2}^n}{\big(P_{O_2}^n+P_{50}^n\big)}, \tag{2.9}$$

where, P_{50} is oxygen partial pressure at 50% haemoglobin saturation and n is the Hill exponent taken as 2.7.

Eqs. (2.7a) and (2.7b) are coupled by using the condition $S_{O_2}=g(P_{O_2})$ as also reported in [38] and the coupled equation is given below:

$$\begin{aligned}&(\alpha_R+[Hb]g'(P_{O_2}))\Big(\frac{\partial P_{O_2}}{\partial t}+\vec{u}\cdot\nabla P_{O_2}\Big)\\&=(\alpha_R D_R+[Hb]D_H g'(P_{O_2}))\nabla^2 P_{O_2}+[Hb]D_H g''(P_{O_2})\big|\nabla P_{O_2}\big|^2.\end{aligned} \tag{2.10}$$

2.2 Initial and boundary conditions

For the plasma velocity, it is assumed no-slip boundary conditions for the top and bottom walls (i.e., $y=b_1$ and $y=b_2$) and the uniform velocity at the inlet and outlet of the capillary

(i.e., $x=a_1$ and $x=a_2$) [16,39]. The initial oxygen partial pressure is uniform throughout the computational domain and it is equal to the mixed-venous oxygen partial pressure (i.e., $P_{O_2}(x,y,0)=P_{\bar{v}O_2}$). The air tissue interfaces (i.e., $y=b_1$ and $y=b_2$) will be at the alveolar oxygen partial pressure (i.e., $P_{O_2}(x,y=b_1,b_2,t)=P_{AO_2}$). The partial pressure P_{O_2} is assumed to be periodic in the flow direction and at the cell plasma boundary both P_{O_2} and normal oxygen flux are continuous [10].

2.3 Numerical method

Next, the numerical calculation procedure to solve above governing equations is presented. First, the governing equations are non-dimensionalized by choosing the appropriate reference values for the variables. The reference velocity is $\bar{V}\equiv$ inlet velocity (1000μm/s), unless mentioned otherwise, the reference pressure is $\bar{p}=\rho\bar{V}^2$ and the reference length is $\bar{r}\equiv$ maximum radius of the cell. The reference time is therefore $\bar{t}=\bar{r}/\bar{V}$, the reference membrane tension is $\bar{T}=E_e$ and the reference value of the oxygen partial pressure is $\bar{P}_{O_2}\equiv$ initial oxygen partial pressure of the cell. Then, the non-dimensional variables are denoted by an asterisk ($*$) mark and the non-dimensional form of Eqs. (2.1a), (2.1b), (2.6), and (2.10) are given below as:

$$\frac{\partial\vec{u}^*}{\partial t^*}+\vec{u}^*\cdot\nabla\vec{u}^*=-\nabla p^*+\frac{1}{\mathrm{Re}}\nabla^2\vec{u}^*+\vec{F}^*, \tag{2.11a}$$

$$\nabla\cdot\vec{u}^*=0, \tag{2.11b}$$

$$\left(\frac{\partial P^*_{O_2}}{\partial t^*}+\vec{u}^*\cdot\nabla P^*_{O_2}\right)=\frac{1}{Pe}\nabla^2P^*_{O_2}, \tag{2.11c}$$

$$\left(\frac{\partial P^*_{O_2}}{\partial t^*}+\vec{u}^*\cdot\nabla P^*_{O_2}\right)=G_1(P^*_{O_2})\nabla^2P^*_{O_2}+G_2(P^*_{O_2})\left|\nabla P^*_{O_2}\right|^2, \tag{2.11d}$$

where, $Re=\rho\bar{V}\bar{r}/\mu$ and $Pe=\bar{V}\bar{r}/D_R$ are the Reynolds and Peclet numbers, respectively, and

$$G_1(P^*_{O_2})=\frac{\alpha_R D_R+[Hb]D_H g'(P_{O_2})}{\bar{V}\bar{r}(\alpha_R+[Hb]g'(P_{O_2}))}\quad\text{and}\quad G_2(P^*_{O_2})=\frac{[Hb]D_H\bar{P}_{O_2}g''(P_{O_2})}{\bar{V}\bar{r}(\alpha_R+[Hb]g'(P_{O_2}))}$$

are two non-dimensional functions.

The equations of motion Eqs. (2.11a) and (2.11b) are solved using a projection method coupled with the IIM as reported in Le et al. [26]. The spatial discretization is carried out on a standard marker-and-cell (MAC) staggered grid [27]. The number of cells in the x and y directions are M and N, respectively. The cell membrane is represented by N_b number of marker points which are called control points. Eqs. (2.11a) and (2.11b) are discretized as

$$\frac{\vec{u}^{*,m+1}-\vec{u}^{*,m}}{\Delta t^*}+\left(\vec{u}^*\cdot\nabla\vec{u}^*\right)^{m+1/2}$$

$$= -\nabla p^{*,m+1/2} + \frac{1}{2Re}\left(\nabla^2 \vec{u}^{*,m+1} + \nabla^2 \vec{u}^{*,m}\right) - Q\{\vec{u}_t^*\}, \tag{2.12a}$$

$$\nabla \cdot \vec{u}^{*,m+1} = 0, \tag{2.12b}$$

where, $Q\{\vec{u}_t\}$ is a temporal correction term to take into consideration the discontinuous or non-smooth velocity distribution across the membrane in the finite difference scheme. The detailed calculation procedure of Eqs. (2.12a) and (2.12b) has been reported in previous works as seen in Jayathilake et al. [28–30] and hence not repeated here. The cell membrane configuration at $t^* = t^{*,m+1} = (m+1)\Delta t^*$ is updated explicitly as $X^{*,m+1} = X^{*,m} + \Delta t^* \cdot U^{*,m}$, $Y^{*,m+1} = Y^{*,m} + \Delta t^* \cdot V^{*,m}$, where $\vec{U}^* = (U^*, V^*)$ is the membrane velocity. Having known the velocity field, the transport equations Eqs. (2.11c) and (2.11d) are discretized explicitly to compute the oxygen distribution in the computational domain. For example, Eq. (2.11d) is discretized at $t^{*,m+1}$ as

$$\left(\frac{P_{O_2}^{*,m+1} - P_{O_2}^{*,m}}{\Delta t^*} + \vec{u}^{*,m} \cdot \nabla P_{O_2}^{*,m}\right) = G_1^m \nabla^2 P_{O_2}^{*,m} + G_2^{m2} |\nabla P_{O_2}^{*,m}|^2. \tag{2.13}$$

3 Results and discussions

Code validations of the present fluid solver have been provided in Jayathilake et al. [28] by simulating the simple shear flow and capsule-substrate adhesion, and hence would not repeated here. In the present work the oxygen transport equations are solved together with the same fluid solver. In the present work, the oxygen uptake by single/multiple stationary cells is examined, and then the oxygen uptake by a single RBC and a single IRBC under flowing condition are investigated separately. The oxygen uptake by the cells and plasma is assessed by computing the following quantities.

(i) The volume averaged oxygen partial pressure inside the cell $P_{cell}(t)$ is given by

$$P_{cell}(t) = \frac{1}{A_{cell}} \int_{cell} P_{O_2}(x,y,t)dxdy, \tag{3.1}$$

where, A_{cell} is the enclosed cross sectional area of the cell.

(ii) The volume averaged haemoglobin saturation inside the cell $S_{cell}(t)$ is given by

$$S_{cell}(t) = \frac{1}{A_{cell}} \int_{cell} S(x,y,t)dxdy. \tag{3.2}$$

(iii) The total increment of the oxygen within the capillary by $t = T$, $M_{O_2}(T)$ is given by

$$M_{O_2}(T) = h \int_{b_1}^{b_2} \int_{a_1}^{a_2} C_{O_2}(x,y,T) - C_{O_2}(x,y,0)dxdy, \tag{3.3}$$

where the oxygen concentration $C_{O_2} = [Hb]S + \alpha P_{O_2}$ for the cell, $C_{O_2} = \alpha P_{O_2}$ for the plasma, and h is the width of the cell. Alternatively, $M_{O_2}(T)$ should be equal to the oxygen

mass transported through the capillary walls due to the conservation of oxygen mass and hence,

$$M_{O_2}(T)=\int_0^T \Psi(t)dt, \tag{3.4}$$

where

$$\Psi(t)=\int_{x=a_1}^{x=a_2} h\alpha_P D_P\Big\{\Big(\frac{\partial P_{O_2}}{\partial y}\Big)_{y=b_2}-\Big(\frac{\partial P_{O_2}}{\partial y}\Big)_{y=b_1}\Big\}dx.$$

3.1 Oxygen uptake by a single stationary cell

The oxygen uptake by a single RBC and a single IRBC located at the center of the computational domain $[-20,20]\times[0,10]\mu$m are separately simulated and compared. The initial shape of the RBC is biconcave [4] and is given by

$$X=a\varphi\sin\chi, \tag{3.5a}$$

$$Y=a\frac{\varphi}{2}(0.207+2.003\sin^2\chi-1.123\sin^4\chi)\cos\chi, \tag{3.5b}$$

where φ is equal to 1.39, χ ranges from -0.5π to 0.5π and a is chosen as 0.72 so that the maximum radius of the RBC is 3μm. The other properties of the RBC are given in Table 1. The computational mesh is $M=256$, $N=64$. The control points N_b for the RBC and the IRBC are 96 and 128, respectively.

For the IRBC, the properties are different from those of the RBC. As the malaria parasite grows in the biconcave RBC, the shape of the IRBC becomes spherical [16, 17]. As

Table 1: The parameters used for the numerical simulation.

	Parameter	Value	Reference
Plasma	α_P	1.4nmol cm^{-3}mmHg^{-1}	[25]
	D_P	2.4×10^{-5}cm^{2}2s^{-1}	[25]
RBC	α_R	1.4nmol cm^{-3}mmHg^{-1}	[25]
	D_R	2.4×10^{-5}cm^{2}2s^{-1}	[25]
	D_H	1.4×10^{-7}cm^{2}s^{-1}	[25]
	$[Hb]$	2.0×10^4nmol cm^{-3}	[25]
	E_e	6×10^{-3}dyne cm^{-1}	[6]
	E_b	1.8×10^{-12} dyne cm	[6]
	n	2.7	[10]
	P_{50}	26mmHg	[10]
Others	ρ	1g cm^{-3}	[6]
	μ	1.2×10^{-2}P	[6]
	h	4.57×10^{-4}cm	
	P_{vO_2}	40mmHg	
	P_{AO_2}	100mmHg	

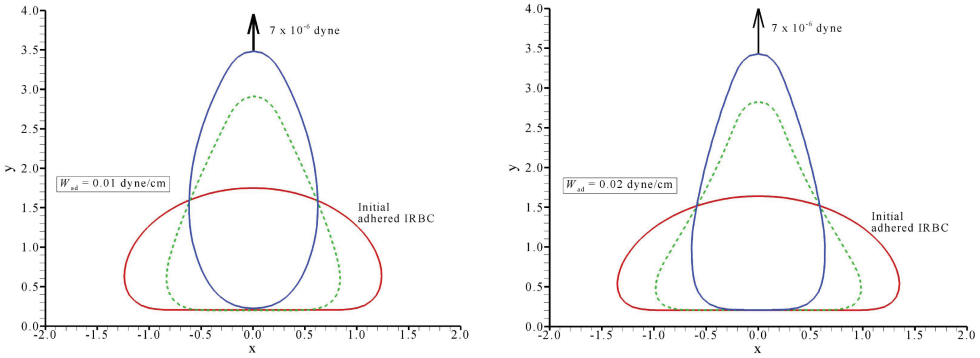

Figure 2: Detachment of the initially adhered IRBC by a pulling force of 7×10^{-6}dyne. (a) $W_{ad}=0.01$dyne/cm; (b) $W_{ad}=0.02$dyne/cm.

such, following Kondo et al. [16], a circular initial shape having the radius of the longitudinal extent of the RBC, which is 3μm, is considered for the IRBC. It is assumed that although the sizes of RBC and IRBC are different, the haemoglobin amount inside each cell is the same unless the haemoglobin is degraded by the malaria parasite. Hence, the haemoglobin bound oxygen, which is significantly larger than the diffused oxygen inside the cell, does not depend on the size of the cell. When a healthy RBC is infected by Plasmodium falciparum, the RBC membrane could be stiffened by a factor of 10 [19,31]. As such the shear modulus of the IRBC membrane is chosen as $E_e=6\times10^{-2}$dyne/cm. The bending modulus of the IRBC is $E_b=1.8\times10^{-12}$dyne cm [19]. Due to the malaria infection, the ODC curve would be right shifted significantly [20,32].Therefore, the parameters of the ODC for IRBC are assumed as $P_{50}=26\text{mmHg}\times1.3(=33.8\text{mmHg})$ and $n=2.7\times0.8(=2.16)$ [32,33]. With development of the malaria parasite inside the cell, the haemoglobin amount decreases [22, 34] since the malaria parasite may ingest between 25% to 75% of the host cell haemoglobin [34,35]. As such, a 65% reduction of haemoglobin is assumed for the IRBC. The other parameters α, D, and D_H for IRBC are assumed to be the same as those values for the RBC, which are given in Table 1. The adhesive coefficient W_{ad} applicable for the IRBC is not known explicitly. As such, it is computed approximately by using the fact that an adhered IRBC is detached by a micropipette aspiration test at a force of 5 to 10×10^{-6}dyne [36]. Therefore, a pulling force of 7×10^{-6}dyne is applied to the initially adhered IRBCs with different applied adhesive coefficients at $W_{ad}=5$,10, and 20×10^{-3}dyne/cm. The pulling force is distributed among six nearby control points around the point the force is applied on the top of the cell. Then, the adhesive coefficient corresponding to the detachment of the IRBC is chosen as the value of W_{ad}. Fig. 2 shows the different shapes of the IRBC at $W_{ad}=10$ and 20×10^{-3}dyne/cm under the applied pulling force; at $W_{ad}=5\times10^{-3}$dyne/cm, the IRBC becomes completely detached under the mentioned pulling force (not shown). As can be seen in Fig. 2(b), the IRBC just about to detach at $W_{ad}=10\times10^{-3}$dyne/cm, and hence it is chosen as the approximate adhesive

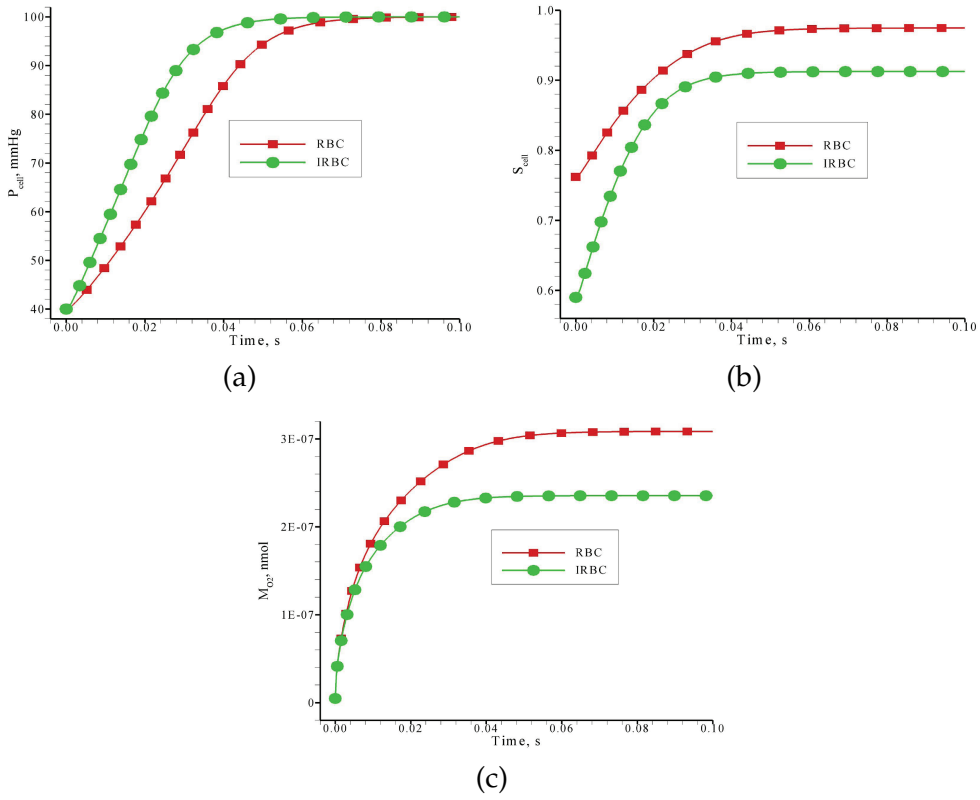

Figure 3: Comparisons the oxygen uptake by RBC and IRBC when both cells are stationary. (a) P_{cell}; (b) S_{cell}; (c) M_{O_2}.

coefficient for the IRBC. It is worth noting that the detached shape shown in Fig. 2(b) concurs reasonably with the detached shape reported experimentally in Nash et al. [36].

Next, the oxygen uptakes are compared in the presence of RBC and IRBC separately when they are located at the center of the computational domain (Fig. 1) and in the absence of a flow field. The initial partial pressure of oxygen in the entire computational domain is uniform at 40mmHg [11]. Fig. 3 shows the variations of the average oxygen partial pressure within the cell, the average oxygen saturation within the cell, and the total quantity of oxygen transported to the capillary as a function of time. As can be seen in Fig. 3(a), the oxygen partial pressure of both the cells reaches the alveolar gas pressure and the IRBC reaches the alveolar gas pressure faster than the RBC does. If the index of the percentage completion of equilibrium of the RBC/IRBC is defined as

$$I_P = \frac{P_{cell} - P_{vo2}}{P_{Ao2} - P_{vo2}} \times 100\%,$$

the RBC and IRBC reach 95% equilibrium (i.e., $I_P = 95\%$) at 0.056 and 0.039s, respectively. A possible explanation is that the oxygen has combined with haemoglobin much faster in

Table 2: Oxygen uptake in the presence of stationary RBC/IRBC.

	t (s)	P_{O_2} (mmHg)	S_{O_2}	O_2 in the cell (nmol)	M_{O_2} (nmol)
RBC	0.1	100	0.97	1.58E-7	3.08E-7
IRBC	0.1	100	0.91	9.28E-8	2.35E-7

the RBC than in the IRBC since the hemoglobin concentration of the RBC is much higher than that of the IRBC. Therefore, free oxygen dissolved in the RBC would be less than that of the IRBC, and hence the oxygen partial pressure of the IRBC is higher than that of the RBC before the equilibrium state is attained. Fig. 3(b) shows that the haemoglobin saturation in the RBC and IRBC are 97% and 91%, respectively. This is due to the fact that the ODC of the IRBC is right-shifted and hence the oxygen saturation of the IRBC is lower compared to the RBC at a given partial pressure of oxygen. As seen in Fig. 3(c), it indicates that more oxygen is potentially transported to the (downstream) capillary in the presence of the RBC. It is found numerically that the amount of oxygen transport to the capillary in the presence of the IRBC is only at best about 76% of the oxygen possible with the presence of the RBC. This is attributed to the haemoglobin content and haemoglobin saturation of the IRBC being lesser and hence its oxygen capacity is lower than that of the RBC. It may be noted, the initial rate of oxygen uptake is fairly similar for the two cases since it takes about $(b_2-b_1)^2/4D_P \approx 0.01$s for oxygen to diffuse from the walls to the respective cell and hence the chemical reaction occurring between the oxygen and haemoglobin within the cell would be delayed. As such, initially, the increment of M_{O_2} is due to the oxygen mass increment in the plasma, which is fairly similar for both cases as the contribution by the haemoglobin is minimal at this stage. A comparison of the numerical values of oxygen uptake for the RBC and IRBC are given in Table 2. It is seen that at the equilibrium the oxygen content in the IRBC is only about 59% of that of the RBC indicating that the oxygen capacity of the IRBC is much lower than that of the RBC.

3.2 Oxygen uptake by multiple stationary cells

Next, three numerical experiments for a cluster of RBCs and IRBCs in the absence of a plasma flow field are performed. The parameters are the same as those with Section 3.1. In the first case (Case 1), five RBCs are included in the above capillary and in the second case (Case 2), four RBCs and one IRBC and in the third case (Case 3), three RBCs and two IRBCs are included as shown in Fig. 4. As shown in Figs. 5(a) and (b), the transient variations of the oxygen partial pressure of RBCs/IRBCs and the haemoglobin saturation are fairly similar to the respective results obtained when stationary RBC and IRBC are located individually in the capillary (Figs. 3(a) and (b)). Here, P_{cell} and S_{cell} have been calculated by taking the average over all RBCs/IRBCs in the capillary. It reveals that the haemoglobin saturation of a RBC/IRBC would not be significantly affected if the RBC/IRBC is included in a cluster of RBCs/IRBCs provided the separation distance is about the dimension of the IRBC or the longitudinal extent of the RBC (It is expected

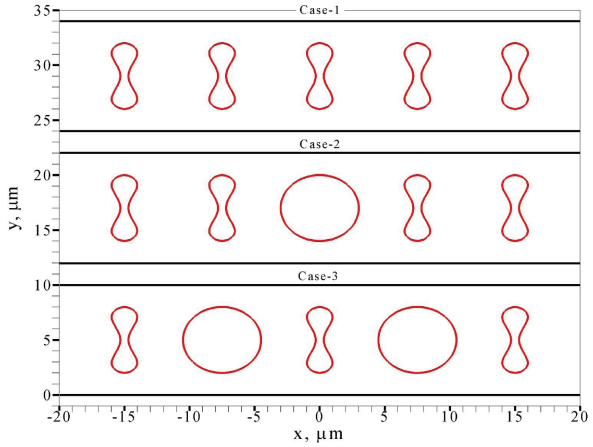

Figure 4: Arrangements of stationary RBCs and IRBCs for Case 1, Case 2, and Case 3.

that as the separation distance between RBC/IRBC becomes much smaller, there will be deviation from the single RBC/IRBC behavior). Moreover, since the oxygen source at the capillary wall is unlimited and basically the oxygen travels in the radial direction of the capillary, the present arrangement of the cells in the axial direction would not affect on the oxygen uptake by individual cell. As seen in Fig. 5(c), the oxygen uptake by the cells and plasma (or capillary) decreases with the number of IRBCs. At each instance as each RBC is replaced by one IRBC, the equilibrium M_{O_2} is reduced by 7.30×10^{-8}nmol (i.e., 8% of the value that obtained for the Case 1). As such, the oxygen capacity of the blood would go down when the malaria parasite invades more healthy red blood cells.

3.3 Oxygen uptake by a single moving cell

All the parameters are the same with that found in Section 3.1 except that now a uniform (inlet/outlet) velocity of $U=1000\mu$m/s is imposed at $x=a_1$ and a_2. Initially, the center of the cell is located at $x=-15\mu$m and the cell is allowed to move along the capillary until $x=16.5\mu$m (say the right end). The initial cell arrangement is at the center of the capillary. Figure 6 shows the axi-symmetric deformation of the RBC and IRBC under the imposed plasma flow field. It is seen that the initial bi-concave RBC reaches a "parachute" shape while the initial circular IRBC reaches an approximate semi-circular shape. The results indicate that both cells move along the capillary at fairly the same velocity since the convective velocity at the center region of the capillary is fairly the same for both cases. Fig. 7 illustrates the quantities of oxygen uptake as the cells move along the centerline of the capillary. Fig. 7(a) shows that oxygen partial pressure of the IRBC increases faster than that of the RBC does. The oxygen partial pressure in the RBC and IRBC when they reach $x=16.5\mu$m is about 64.67 and 83.34mmHg (or $I_P=41\%$ and 72%), respectively. As seen in Fig. 7(b), the RBC and IRBC are saturated by oxygen at about 92% and 83%, respectively, when they reach the right end. As similarly shown in Fig. 3(b) for the stationary cell-

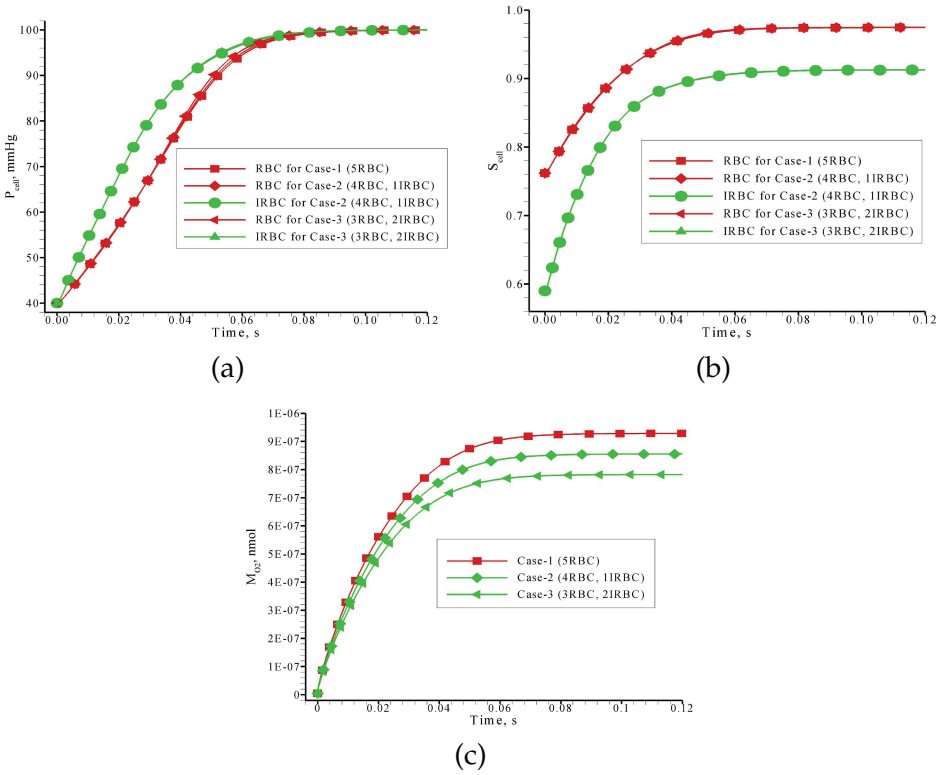

Figure 5: Comparisons the oxygen transport when five cells are stationary (Case 1, Case 2, and Case 3). (a) P_{cell}; (b) S_{cell}; (c) M_{O_2}.

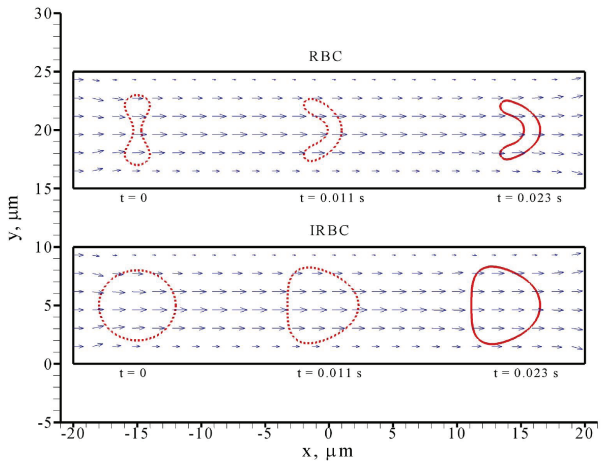

Figure 6: Deformation of cells and the velocity fields when the cells reach x=16.5μm. when the cells are initially at the center.

s, the oxygen saturation of the IRBC is less than that of the RBC. Furthermore, Fig. 7(c) shows that during the selected time period more oxygen is transported downstream of

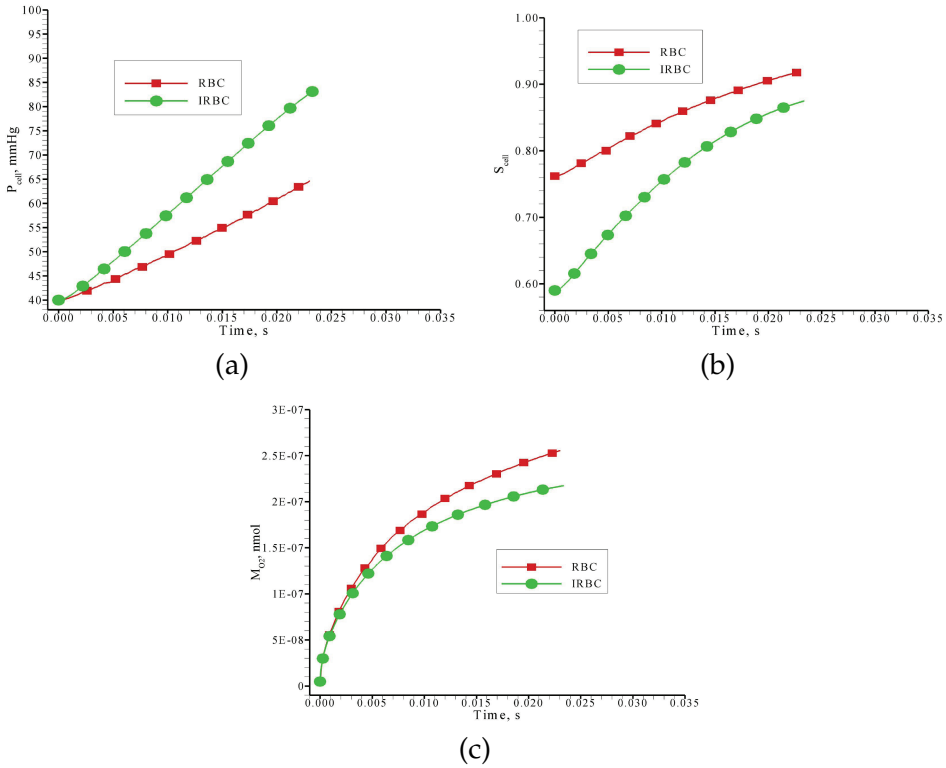

Figure 7: Comparisons for the oxygen transport in the presence of RBC and IRBC when both cells are moving along the centerline of the capillary. (a) P_{cell}; (b) S_{cell}; (c) M_{O_2}.

the capillary in the presence of the RBC on comparison to the IRBC.

Next, the above experiment is performed when the cells are initially placed near to one wall of the capillary in which cell-wall adhesion would affect on cell motion and oxygen uptake. In Fig. 8, it is seen that the RBC gradually moves away from the wall and reaches near to the centerline of the capillary which is called cell migration as seen in [11]. However, the IRBC does not move away from the wall; instead the IRBC rolls along the capillary wall due to the interaction between the cell membrane and the capillary wall. It is noted that this rolling behavior of the IRBC agrees with other findings [16]. The results show that as the RBC moves away from the wall and towards the center region of the capillary, the larger convective velocity enables it to move faster downstream as compared to the IRBC; the slower convective velocity closer to the wall has led to the IRBC to assume a lower speed downstream. Moreover, the results show that the RBC reaches the right end almost at the same time for either initial position. However, the IRBC is delayed time-wise by about 30% to reach the right end when it moves near to one wall. Fig. 9 demonstrates the quantities of oxygen uptake when the cell is initially located near to one wall. As seen in Fig. 9(a), the increment of the oxygen partial pressure in the IRBC is faster than that of the RBC as similarly seen above for Fig. 7(a). The partial

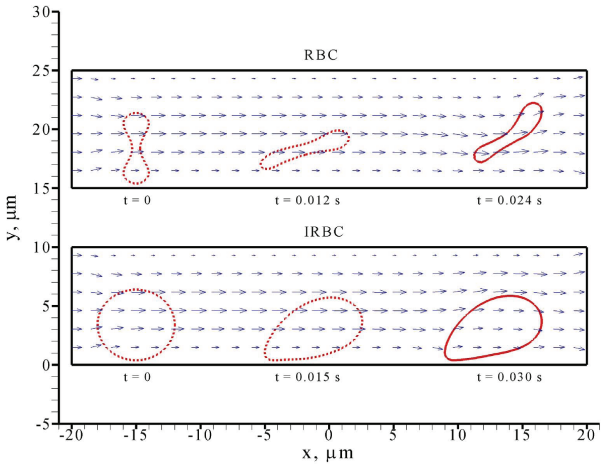

Figure 8: Deformation of cells and the velocity fields when the cells reach $x=16.5\mu$m. when the cells are initially near to one wall.

pressures when the RBC and IRBC reach the right side are 69.67 and 95.94 mmHg (or $I_P=49\%$ and 93%), respectively. It is clear that the cells do not reach the alveolar oxygen partial pressure (100mmHg) when they reach the right end of the capillary. To complete the oxygen uptake (i.e., $I_P=100\%$) by the moving cells as seen for the stationary cells, the moving cells have to be allowed to move more distance along the capillary or the inflow velocity has to be reduced so that the cells could spend more time on the capillary.

A RBC typically resides in the pulmonary capillary for about 0.75s [37], and hence the RBC could easily complete the oxygen uptake before leaving the pulmonary capillary. The oxygen saturation and the total oxygen uptake of RBC and IRBC shown in Figs. 9(b) and (c) have correspondingly similar trends as the respective plots obtained for the cells moving along the centerline (i.e., Figs. 7(b) and (c)). For ease of comparison, the oxygen uptake M_{O_2} for stationary and moving cells are compared at $t=0.02$s. The oxygen uptake M_{O_2} for the moving RBC and IRBC when cells are moving near to the centerline are, respectively, 100% and 87% of that of the stationary RBC (Fig. 3(c)). If the cells move near to one wall, M_{O_2} for the moving RBC and IRBC are, respectively, 105% and 90% of that of the stationary RBC. When the cells move near to one wall the oxygen uptake increases slightly because the cells are closer to the oxygen source, which is the capillary wall. By comparing Figs. 3, 7 and 9, it shows that the rate of oxygen uptake by the capillary is fairly similar between the cases of stationary cells and moving cells. This suggests that the oxygen uptake by both RBC and IRBC is probably dominated by the diffusion over the convection effect although the Peclet number is of the order of unity for the present problem. Whiteley et al. [11] has previously reported that the convective term has negligible effect on the oxygen uptake by RBC since the term $\vec{u}\cdot\nabla P_{O_2}$ would be very small for this problem. As such, Fig. 3(c) suggests that the RBC and IRBC would complete oxygen uptake (i.e., $I_P=100\%$) if they continue the downstream motion another span of the same

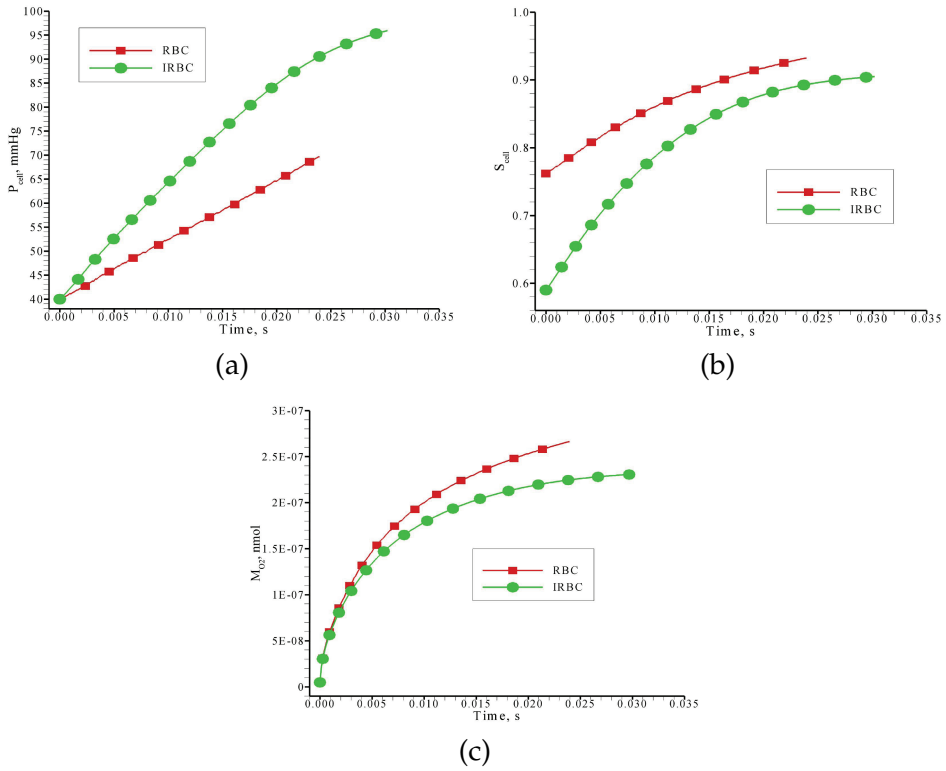

Figure 9: Comparisons for the oxygen transport in the presence of RBC and IRBC when both cells are initially near to one wall of the capillary. (a) P_{cell}; (b) S_{cell}; (c) M_{O_2}.

capillary for the chosen inflow velocity. Even though the RBC and IRBC would complete oxygen uptake when they leave the capillary due to the fact that each cell resides on capillary for about 0.75s, it should be noted that the oxygen uptake by the IRBC is lower than that of the RBC as seen in Fig. 3(c). Although the mass convection would not have significant effects on oxygen uptake by RBCs/IRBCs in the radial direction of the capillary (the y direction), the convection is very important to carry the oxygen from lungs to other parts of the body (in the x direction). Moreover, Table 3 shows a comparison for the total oxygen uptake by the moving cells when they reach the right end of the capillary. It is seen that the oxygen content in the IRBC is significantly lower than that of the RBC.

Table 3: Oxygen uptake in the presence of moving RBC/IRBC.

		t (s)	P_{O_2} (mmHg)	S_{O_2}	O_2 in the cell (nmol)	M_{O_2} (nmol)
Center	RBC	0.023	64.67	0.92	1.15E-07	2.56E-7
	IRBC	0.023	83.34	0.87	8.03E-8	2.17E-7
Wall	RBC	0.024	69.67	0.93	1.25E-7	2.66E-7
	IRBC	0.030	95.94	0.90	9.01E-8	2.31E-7

4 Conclusions

The IIM is used to model the oxygen uptake by RBCs/IRBCs when it passes through a tiny capillary in the lungs. Some numerical experiments are performed to examine the effect of malaria infection on oxygen uptake by RBCs.

When both cells are stationary, it is seen that the IRBC reaches the alveolar oxygen partial pressure faster than the RBC does and the haemoglobin saturation of IRBC is lesser than that of the RBC. The total oxygen uptake by the capillary is significantly deteriorated in the presence of IRBCs. When a plasma velocity of 1000μm/s is imposed, the oxygen partial pressure of both cells does not reach the alveolar oxygen partial pressure and the haemoglobin is not saturated by oxygen when the cells move within the selected length (40μm) of the capillary. In addition, the present results show that a single RBC/IRBC motion or its deformation does not significantly affect the oxygen uptake by the cell. However, the RBC/IRBC motion helps to transport the oxygen from lungs to the other parts of the body. Moreover, if the numbers of IRBC increases, the oxygen capacity of the blood would go down significantly. Therefore, it is important to find effective treatment methods to overcome this low oxygen capacity of the blood in malaria patients. Exchange transfusion is one established method to improve the quality of the blood. Furthermore, the knowledge of the initial loading phase of oxygen reported in this paper would be important when optimizing the designing of artificial lungs.

The present model is only a simple model to simulate oxygen uptake by RBCs/IRBCs. Our future research is to include different viscosities for the plasma and the intracellular fluid (cytosol). It is also important to study the effect of matured malaria parasite inside the IRBC for the reason that the rigid parasite inside the cell would increase the bond lifetime and decrease the rolling velocity as can be seen in [39]. Furthermore, RBCs and IRBCs remain in the plasma as clusters, and hence IRBCs would likely adhere to healthy RBCs and endothelium and consequently the flow resistance for the blood would increase significantly or even the vascular lumen would be blocked. As such, the oxygen supply to the tissues would be further deteriorated due to the adhesiveness of the membrane, and hence it is important to study this. In the immediate future work, the present calculation is to be extended to the three-dimension using the immersed boundary method (IBM). The fact that the oxygen partial pressure is continuous across the cell membrane is an advantage when the IBM is used.

Acknowledgements

Tan's research was partially supported by the NSFC (Nos. 91230108, 11101446), the Project of Science and Technology New Star of Zhu Jiang in Guangzhou city (No. 2011J2200099), the Specialized Research Fund for the Doctoral Program of Higher Education (No. 20110171120048), Guangdong Natural Science Foundation (No. S2013010012250), the Fundamental Research Funds for the Central Universities

(No. 13lgzd07), Guangdong Provincial Government of China through the "Computational Science Innovative Research Team" program, and Guangdong Province Key Laboratory of Computational Science at the Sun Yat-sen University.

References

[1] T. W. SECOMB AND R. SKALAK, *A two-dimensional model for capillary flow of an asymmetric cell,* Microvasc. Res., 24(1982), pp. 194–203.
[2] T. W SECOMB, *Flow-dependent rheological properties of blood in capillaries,* Microvasc. Res., 34 (1987), pp. 46–58.
[3] C. POZRIKIDIS, *Orbiting motion of a freely-suspended spheroid near a plane wall*, J. Fluid Mech., 541 (2005), pp. 105–114.
[4] C. POZRIKIDIS, *Effect of surfactants on film flow down a periodic wall*, J. Fluid Mech., 496 (2003), pp. 105–127.
[5] Y. LIU AND W. K. LIU, *Rheology of red blood cell aggregation by computer simulation,* J. Comput. Phys., 220(1) (2006), pp. 139–154.
[6] J. ZHANG, P. C. JOHNSON AND A. S. POPEL, *Red blood cell aggregation and dissociation in shear flows simulated by Lattice Boltzmann method,* J. Biomech., 41(1) (2008), pp. 47–55.
[7] D. HARTMANN, *A multiscale model for red blood cell membranes,* Biomech. Model. Mechanobiol., 9 (2010), pp. 1–17.
[8] J. D. HELLUMS, *The resistance to oxygen transport in the capillaries relative to that in the surrounding tissue,* Microvasc. Res., 13 (1997), pp. 131–136.
[9] K. GROEBE AND G. THEWS, *Effects of red cell spacing and red cell movement upon oxygen release under conditions of maximally working skeletal muscle,* Adv. Exp. Med. Biol., 248 (1989), pp. 175–185.
[10] C. WANG AND A. S. POPEL, *Effect of red blood cell shape on oxygen transport in capillaries,* Math. Biosci., 116 (1993), pp. 89–110.
[11] L. SHI, T.-W. PAN AND R. GLOWINSKI, *Numerical simulation of lateral migration of red blood cells in Poiseulille flows,* Int. J. Numer. Meth. Fluid, 68 (2012), pp. 1393–1408.
[12] S. P. DAVIS, M. AMREIN, M. R. GILLRIE, K. LEE, D. A. MURUVE AND M. HO, *Plasmodium falciparum-induced CD36 clustering rapidly strengthens cytoadherence via p130CAS-mediated actin cytoskeletal rearrangement,* FASEB J., 26 (2012), pp. 1119–1130.
[13] A. M. DONDORP, P. A. KAGER, J. VREEKEN AND N. J. WHITE, *Abnormal blood flow and red blood cell deformability in severe malaria,* Parasitol. Today, 16(6) (2000), pp. 228–232.
[14] M. HO AND N. J. WHITE, *Molecular mechanics of cyto-adherence in malaria,* Am. J. Physiol. Cell Ph., 276 (1999), pp. 1231–1242.
[15] J. P. SHELBY, J. WHITE, K. GANESAN, P. K. RATHOD AND D. T. CHIU, *A microfluidic model for single-cell capillary obstruction by Plasmodium falciparum infected erythrocytes,* Proc. Nat. Acad. Sci. USA, 100(25) (2003), pp. 14618–14622.
[16] T. KONDO, Y. IMAI, T. ISHIKAWA, K. TSUBOTA AND T. YAMAGUCHI, *Hemodynamics analysis of microcirculation in malaria infection,* Ann. Biomed. Eng., 37 (2009), pp. 702–709.
[17] Y. IMAI, K. NAKAAKI, H. KONDO, T. ISHIKAWA, C. T. LIM AND T. YAMAGUCHI, *Margination of red blood cells infected by Plasmodium falciparum in a microvessel,* J. Biomech., 44 (2011), pp. 1553–1558.
[18] T. W. SECOMB, R. HSU AND A. R. PRIES, *A model for red blood cell motion in glycocalyx lined capillaries,* Am. J. Physiol. Heart C, 274 (1998), pp. 1016–1022.

[19] D. A. FEDOSOV, B. CASWELL AND G. E. KARNIADAKIS, *Wall shear stress-based model for adhesive dynamics of red blood cells in malaria,* Biophys. J., 100 (2011), pp. 2084–2093.
[20] S. KRISHNA, E. A. SHOUBRIDGE, N. J. WHITE, D. J. WEATHERALL AND G. K. RADDA, *Plasmodium yoelii: Blood oxygen and brain function in the infected mouse,* Exp. Parasitol., 56 (1983), pp. 391–396.
[21] J. J. SCHALL, A. F. BENNETT AND R. W. PUTNAM, *Lizards infected with malaria: Physiological and behavioral consequences,* Science, 217 (1982), pp. 1057–1059.
[22] J. BONGBELE, A. EWAMELA, E. DIAKOUNDILA AND R. MANKELE, *Oxygen transport capacity of blood in athletes with malarial infection,* Rev. Mal. Respir., 15(1) (1998), pp. 57–59.
[23] R. J. LEVEQUE AND Z. LI, *The immersed interface method for elliptic equations with discontinuous coefficients and singular sources,* Siam J. Numer. Anal., 31 (1994), pp. 1019–1044.
[24] U. SEIFERT, *Adhesion of vesicles in the two dimensions,* Phys. Rev. A, 43 (1991), pp. 6803–6814.
[25] A. O. FRANK, C. J. C. CHUONG AND R. L. JOHNSON, *A finite-element model of oxygen diffusion in the pulmonary capillaries,* J. Appl. Physiol., 82 (1997), pp. 1717–1718.
[26] D. V. LE, B. C. KHOO AND J. PERAIRE, *An immersed interface method for viscous incompressible flows involving rigid and flexible boundaries,* J. Comput. Phys., 220 (2006), pp. 109–138.
[27] J. KIM AND P. MOIN, *Application of a fractional step method to incompressible Navier-Stokes equations,* J. Comput. Phys., 59 (1985), pp. 308–323.
[28] P. G. JAYATHILAKE, G. LIU, ZHIJUN TAN AND B. C. KHOO, *Numerical study of a permeable capsule under Stokes flows by the immersed interface method,* Chem. Eng. Sci., 66(10) (2011), pp. 2080–2090.
[29] P. G. JAYATHILAKE, B. C. KHOO AND ZHIJUN TAN, *Effect of membrane permeability on capsule substrate adhesion: computation using immersed interface method,* Chem. Eng. Sci., 65(11) (2010a), pp. 3567–3578.
[30] P. G. JAYATHILAKE, ZHIJUN TAN, B. C. KHOO AND N. E. WIJEYSUNDERA, *Deformation and osmotic swelling of an elastic membrane capsule in Stokes flows by the immersed interface method,* Chem. Eng. Sci., 65(3) (2010b), pp. 1237–1252.
[31] S. SURESH, J. SPATZ, J. P. MILLS, A. MICOULET, M. DAO, C. T. LIM, M. BEIL AND T. SEUFFERLEIN, *Connections between single-cell biomechanics and human disease states: gastrointestinal cancer and malaria,* Acta. Biomater., 1 (2005), pp. 15–30.
[32] P. SASI, S. P. BURNS, C. WARUIRU, M. ENGLISH, C. L. HOBSON, C. G. KING, M. MOSOBO, J. S. BEECH, R. A. ILES, B. J. BOUCHER AND R. D. COHEN, *Metabolic acidosis and other determinants of hemoglobin-oxygen dissociation in severe childhood Plasmodium falciparum malaria*, Am. J. Trop. Med. Hyg., 77(2) (2007), pp. 256–260.
[33] N. A. STATHOPOULOS, P. K. NAIR AND J. D. HELLUMS, *Oxygen transport studies of normal and sickle red cell suspensions in artificial capillaries,* Microvasc. Res., 34 (1987), pp. 200–210.
[34] D. E. GOLDBERG, A. F. G. SLATER, A. CERAMI AND G. B. HENDERSON, *Hemoglobin degradation in the malaria parasite Plasmodium falciparum: An ordered process in a unique organelle,* Proc. Nat. Acad. Sci. USA, 87 (1990), pp. 2931–2935.
[35] V. L. LEW, T. TIFFERT AND H. GINSBURG, *Excess hemoglobin digestion and the osmotic stability of Plasmodium falciparum-infected red blood cells*, Blood, 101 (2003), pp. 4189–4194.
[36] G. B. NASH, B. M. COOKE, K. MARSH, A. BERENDT, C. NEWBOLD AND J. STUART, *Rheological analysis of the adhesive interactions of red blood cells parasitized by Plasmodium falciparum,* Blood, 79 (1992), pp. 798–807.
[37] J. F. NUNN, Applied Respiratory Physiology, Butterworth-Heinemann, Oxford, UK, 1993.
[38] J. P. WHITELEY, D. J. GAVAGHAN AND C. E. W. HAHN, *Some factors affecting oxygen uptake by red blood cells in the pulmonary capillaries*, Math. Biosci., 169 (2001), pp. 153–172.

[39] N. A. N'DRI, W. SHYY AND R. TRAN-SON-TAY, *Computational modeling of cell adhesion and movement using a continuum-kinetics approach,* Biophys. J., 85 (2003), pp. 2273–2286.